

PROPRIETĂȚILE ȘI CARACTERISTICILE MICROSTRUCTURALE ALE UNOR LIANȚI MICȘTI CU ZGURĂ, ACTIVAȚI ALCALIN PROPERTIES AND MICROSTRUCTURAL CHARACTERISTICS OF ALKALI-ACTIVATED SLAG-BLENDED CEMENTS

N.R. RAKHIMOVA*,

Kazan State University of Architecture and Engineering, Department of Building Materials
420043, Russian Federation, Kazan, Zelenaya Str. 1

The effects of ground used sand (GUS), ground fly ash (GFA) (class F), and microsilica (MS) on water requirement, setting time, and compressive and bending strength development of alkali-activated slag-blended cements (AASBC) were studied. Siliceous blending materials were found to be able to replace up to 50% of ground granulated blast furnace slag (GGBFS) and contributed to up to 90% improvement of strength of AASBCs. The granulation for GUS, granulation, curing conditions, and basicity of GGBFS for GFA, and curing conditions for MS have effects on the development of the properties of the AASBCs.

Keywords: Blast furnace slag, alkalis, activators, binding composite materials, setting time, mechanical properties

1. Introduction

Sustainable development in the construction industry requires effective blended cements and materials based on these blended cements. The introduction of supplementary cementitious materials (SCM) in traditional and alternative cements, in addition to solving imperious ecological problems, also improves the performance capabilities of the cement.

Extensive literature on the research and application of blended ordinary Portland cements (OPC) is available; however, the potential of the combination of various types of SCMs and OPC are yet to be exhaustively studied and reported. Further, sustainability in this field is associated with an increasing use of known SCMs, development and use of new SCMs, and the development and use of different clinker types. This requires a scientific approach to understand the reactions and performance of such materials combination [1].

SCMs are classified into two types, inert and active, which are the most frequently used classifications in building materials science. It is usually to name mineral powders that react with OPC and water as reactive SCMs, and those that do not form hydration products with binding properties as inert SCMs or simply fillers because of the insignificant interaction of the cement paste with such materials. This distinction is clearly relative because all types of mineral powders have some degree of effect on the structure and properties of mixed binders and therefore, in addition to being active, they are also multifunctionally active, differing only in the mechanism of influence on the structure and

properties of the filled binders. Therefore, it seems reasonable to classify mineral blending materials based on whether they are “chemically active” i.e. they form hydration products with cementitious properties or are “physically active” i.e. they do not form hydration products. The “physically active” mineral blending materials affect the physical structure and properties of blended binders, i.e. they are “physically active and reactive” supplementary materials and they combine both “filler” and “modifier” effects [2].

This approach is very reasonable for alkali-activated slag-blended cements (AASBC). The substitution and modifications represent the most promising trend for alkali-activated slag cements (AASC). Alkali activation allows for effective interaction between the AASC paste, fillers, and modifiers and enhances the compatibility with mineral blending materials of various compositions and structures. Hence, a much wider range of various mineral materials are usable with AASBCs than with blended OPCs. Therefore, the properties of AASCs are dependent on many more factors than OPCs. In addition to the influencing factors common to all powdery binders, i.e. chemical and mineralogical composition, fineness, water/binder ratio, and curing conditions, the influencing factors related to the alkaline component, its composition, and concentration, have a significant effect on the properties and structure of the AASCs.

Influencing factors of blending materials for AASBC are similarly to those for OPCs, and they include composition, fineness, and the amount of glassy phase. Due to the diverse range of SCMs used, generic relations between the composition,

* Autor corespondent/Corresponding author,
E-mail: rahimova.07@list.ru

particle size, and exposure conditions, such as temperature or relative humidity become increasingly crucial [3].

Some of the main influencing factors controlling AASBC and their significance have been investigated. In this aspect, alkali-activated slag-fly ash systems have been most extensively researched.

Smith and Osborne [4] were the first which reported on alkali-activated slag-fly ash systems. A combination of 60% slag and 40% fly ash with 7% NaOH (relative to the combined mass of slag and fly ash) showed good early mechanical strengths and a small strength gain after 28 days.

Tang [5] investigated the effect of slag/fly ash ratio, water/binder ratio and activator (waterglass and NaOH) dosage on the strength development of alkali-activated slag-fly ash cements using the factorial design method. He found that these factors affected the strength of the cement in the following order: slag/fly ash ratio > water/binder ratio > waterglass dosage > NaOH dosage.

The activation of fly ash/slag pastes with NaOH solutions have been studied by Puertas [6]. The ratio of fly ash/slag and the activator concentration were found to be significant influence factors. The influence of curing temperature on the development of the strength of the pastes was lower than the contribution of other factors.

The effect of the fineness of ground fly ash with a specific surface area 400 m²/kg on the properties of alkali-activated mortars was studied by Lu C. [7]. Mixed AASC showed a 28-day strength of 76 MPa for a fly ash content of 60%. When non-ground fly ashes were used, the 28-day strength was only approximately 12.9–16.2 MPa.

Partial replacement of the ground granulated blast furnace slag GGBFS by fly-ash gives positive results in improvement of performance capabilities and substitution of slag. Proper slag/fly ash ratio was found to have an effect of a mutual complement to the superiority supplement [8]. Alkali-activated slag-fly ash cements showed very good resistance to acidic, sulphate, and seawater attacks, and corrosion resistance increased with increase in the fly ash replacement [9], which also improved the mechanical strength and pore structure [8, 10–12].

Many studies have demonstrated the complex microstructure and chemical composition of alkali-activated slag-fly ash cements binder gels. Shi and Day [13] and Puertas and Fernandez-Jimenez [14, 15] reported that the main hydration products of alkali-activated slag-fly ash cements were C–S–H and alkali aluminosilicate hydrate gels. Yang found that the microstructure and chemical composition of such blended binders fall between those of the aluminosilicate gel formed in the silicate-activated fly ash and those of calcium

silicate hydrate gel formed in silicate-activated granulated blast furnace slag (GBFS) [16].

Thus, the microstructure, composition, properties, slag/fly ash ratio, water/binder ratio, alkali activator dosage, grinding fineness up to 400 m²/kg, and curing temperature have been investigated as influencing factors for alkali-activated slag-fly ash cements. The influencing factors and their significance in AASBC with “physically active” and “chemically active” blending materials, to the best of our knowledge, have not been reported. In addition, the relevance of the above mentioned influencing factors and the fineness of grinding up to specific surface areas of 800 m²/kg, GGBFS basicity, and pre-hardening time on the property evolution and their dependence on the activity of the blending materials is not completely known. In the present study, we have studied the effect of the typically physically active blending materials, such as silica sand, which is physically active and reactive, fly ash and reactive mineral additions, and microsilica on the properties of fresh and hardened pastes of AASBCs. In addition, we have also attempted to determine the significance of the influencing factors on the property evolution of AASBC. Further, we have attempted to describe the main structural characteristics of AASBCs depending on the activity type of the blending materials.

2. Experimental

The starting materials were ground granulated blast furnace slags (GGBFS) from Orsko-Khalilovsky (GGBFS 1) and Chelyabinsky (GGBFS 2). Specific surface areas (S_{sp}) of the GGBFS were 300 m²/kg. As the blending materials were used industrial by-products of siliceous composition, which in accordance with the proposed classification, can be considered as physically active, physically active and reactive, and reactive i.e. ground used sand (GUS), ground fly ash (GFA), and microsilica MS (Table 1, 2). The GBFSs, used sand (US), and fly ash (FA) were ground in the laboratory planetary mill.

The alkaline activation of the mixed cement was carried out using a commercial sodium carbonate solution. The addition of the alkali activator was adjusted to 5 wt% (by Na₂O) of the blended cement.

The AASBC cement pastes were prepared in cubic moulds (2 × 2 × 2 cm³), cement-sand mortars in prismatic moulds (4 × 4 × 16 cm³). The compressive strength of AASBC was measured after 1, 3, 7, 28, and 365 days of storage under normal conditions (room temperature, humidity 95–100%) and after steam curing regime for 4 + 3 + 6 + 3 h (four hours of pre-hardening time at room temperature, three hours of temperature rise time, six hours of constant temperature 90–95 °C time, and three hours of temperature decrease time).

Table 1

Starting material	Chemical composition of GBFSs and FA										
	Component (mass % as oxide)										
	SiO ₂	CaO	Al ₂ O ₃	MgO	MnO	Fe ₂ O ₃	TiO ₂	Na ₂ O	K ₂ O	P ₂ O ₅	SO ₃
GGBFS 1	40.02	42.02	8.22	6.26	0.34	<0.1	0.36	0.44	0.66	0.04	1.45
GGBFS 2	37.49	36.22	11.58	8.61	0.50	0.16	1.80	0.64	0.95	0.01	2.00
FA (class F)	58.76-62.1	6.12-8.64	15.46-19.31	1.01-2.78	0.09-0.55	7.36-9.33	0.23-0.95	0.35-0.97	0.56-1.05	0.05-0.09	0.17-0.98

Table 2

Characteristics of the blending materials				
Blending material	Content of SiO ₂ , %	Content of amorphous phase, %	S _{sp} , m ² /kg	Mineral composition
GUS	90.1-96.5	0	200-800	quartz
GFA	58.76-62.1	65	200-800	quartz – 7-11%, mullite – 15-18%, Fe-spinel – no more than 5%
MS	93.9-94.7	100	15 000 - 25 000	quartz

Table 3

The characteristics of the fresh paste of the AASBCs with GFA and GUS as blending materials										
Blending material	Content of blending material in AASBC, %	S _{sp} of blending materials, m ² /kg								
		200			500			800		
		Normal consistency, %	Setting time, hour-minute		Normal consistency, %	Setting time, hour-minute		Normal consistency, %	Setting time, hour-minute	
			initial	final		initial	final		initial	final
-	0	24.9	1-20	3-50	24.9	1-20	3-50	24.9	1-20	3-50
GUS	20	24.9	1-10	3-40	25.3	1-20	3-50	25.5	1-40	4-10
	40	24.8	1-50	4-20	25.7	2-20	5-00	26.1	2-50	5-30
	60	24.8	3-00	5-50	26.1	3-50	7-00	26.7	4-40	8-20
GFA	20	27,2	2-00	4-40	27,4	3-00	5-30	28,1	3-50	6-20
	40	29,4	3-50	6-40	29,9	8-20	11-30	31,3	9-40	14-20
	60	31,6	6-40	10-20	32,3	-	-	34,5	-	-

The effectiveness of the blending materials was evaluated by the effectiveness factor (F_e), which is the ratio of the 28-days strength of the specimen obtained by replacing the GBFS by blending materials to that of the reference specimen based on GBFS.

3. Results and discussion

First, the grindability of the starting materials was studied. Figure 1 shows the time necessary for grinding the GBFS to achieve a S_{sp} of 300m²/kg and for US and FA to achieve a S_{sp} of 800m²/kg.

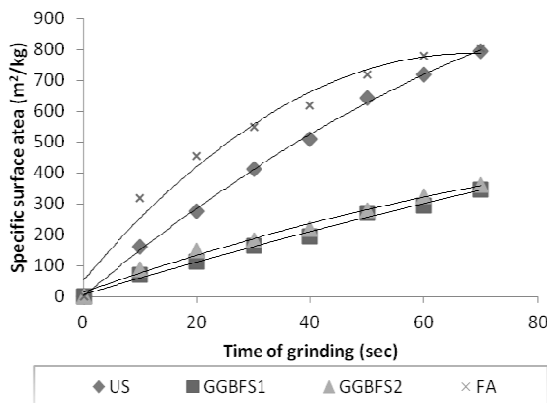


Fig. 1 - Relationships between S_{sp} of the starting materials and time of grinding.

3.1. Physically active GUS

The influence of the GUS on the AASBC fresh paste.

The water requirement of the AASC does not increase when GUS with a S_{sp} of 200 m²/kg is added (AASBC (GUS)) and when the GUS content is increased up to 60%. The introduction of GUS of 500 and 800 m²/kg up to 60% increases the water requirement from 24.9 to 26.1 and 26.7%, respectively. The setting time of AASBC (GUS) with GUS content of up to 20% does not change or is slightly reduced. With increase in the content to up to 60%, due to dilution effect, the setting time is extended by 2–3 times (Table 3).

Influence of the GUS on the AASBC hardened paste

Figures 2–4 show the influence of the blending materials on the compressive strength and its development. Replacement of the GGBFS with GUS (Figure 2) is beneficial, although the AASBC is based on the neutral or acidic GGBFS and is activated by a mildly active non-silicate alkali activator i.e. a sodium carbonate solution. The compressive strength of the AASBC (GUS) samples increases with increase in the basicity of the GGBFS and of curing temperature. A main influencing factor responsible for the maximum

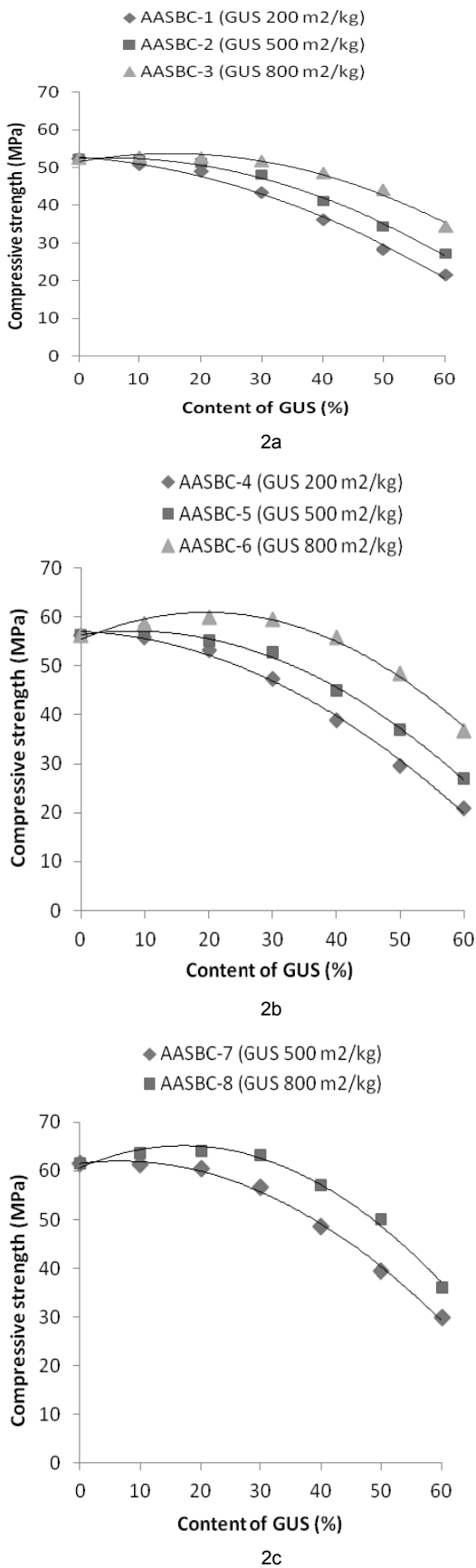


Fig.2 - The variation of the compressive strength of AASBCs (GUS) with S_{sp} , content of GUS, and curing conditions: a) GGBFS1, normal conditions, b) GGBFS1, steam cutting, c) GGBFS2, steam curing.

possible GUS content and its influence on AASBC (GUS) is the fineness of GUS. On the basis of Figure 2, the positive influence of GUS is manifested when S_{sp} exceeds the GGBFS S_{sp} (AASBC-2,3,5-8) by 1.6 times. This can be attributed to several reasons. First, the GUS size particle reduction leads to surface layer amorphization and increases the superficial energy. Secondly, there is an improvement in the grain-size composition of the mixed cement. The amount of particles smaller than 5 μ m increases and is more than 30% [17] when the GUS is ground from 200 to 500-800 m^2/kg (by 4.5 times). The grain-size distribution of the GGBFS at an S_{sp} of 300 m^2/kg is not optimum and improves when particles with sizes lesser than 20 μ m are introduced [18]. Introduction of GUS with the optimum dispersion increases the compressive strength of the hardened paste up to 14% (effective content of GUS = 0–30%) depending on the dispersion of GUS and allows to substitute the GGBFS up to 50%, while maintaining the strength at the level of the reference sample (permissible content of GUS = 0–50%).

The important characteristic of the applicability of supplementary cementitious materials is their effect on the long-term strength development. The results in Figures 3 and 4 indicate that the substitution of GGBFS with 30% GUS ($S_{sp} = 500 m^2/kg$) reduces the compressive strength. Samples of the blended cements hardened 3–7 days show strengths lower than that of the reference samples by up to 20%. The strengths of the blended cements hardened 28 days are very close to that of the reference, and strengths of the samples after 360 days exceed the reference value. An increment in the strength after one year is 10.8–36.7% for the reference sample and 18.4–48% for blended cements (Figure 4).

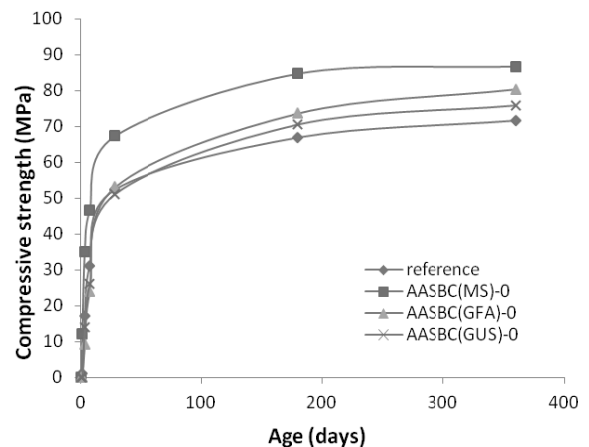


Fig. 3. - Development of the compressive strength of the AASBCs in comparison to the reference up to after 28 days (a) and 360 days (b).

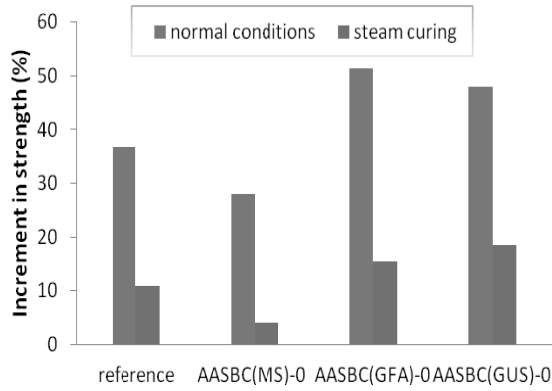


Fig. 4. - Increment in the strength after one year of the AASBCs depending on the curing conditions and type of admixture.

According to Glukhovskiy [19], Shi et al. [20], Deja [21], Xu et al. [22] AASC materials are characterized by dense and uniform interfacial transitional zone between the aggregate and AASC. Our results seem to indicate that the

strengthening of the interfacial transitional zone in AASBCs (GUS) with time substantially contributes to the long-term strength development. Figure 5 shows the amorphous phase of the hardened AASC(GUS) paste, GUS particle, and interfacial zones in between.

The effect of the influencing factors on the efficiency of the GUS follows the order: S_{sp} of GUS > (GGBFS basicity, curing conditions, etc.), F_e of GUS = 0.9–1.14.

The compressive and bending strengths of mortars AASBC(GUS)-0 (Tables 4 and 5) show the maintenance of the compressive strength at the level of the reference sample and a decrease in the bending strength and ratio of compressive strength/bending strength.

3.2. Physically active and reactive GFA

The influence of the GFA on the AASBC fresh paste

The addition of GFA results in an increase in the water requirement and this increase depends

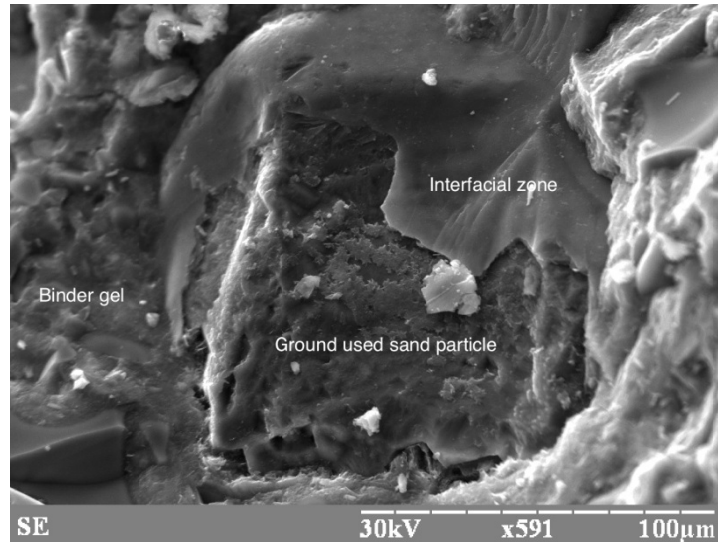


Fig. 5 - Scanning electron image of the hardened AASBC(GUS) paste.

Table 4

Type of AASBC	GGBFS	Admixture	Content of admixture, %	S_{sp} of the admixture
AASBC(GUS)-0	GGBFS1	GUS	30	500
AASBC(MS)-0	GGBFS1	MS	3	15000-25000
AASBC(GFA)-0	GGBFS1	GFA	30	500

Table 5

Type of AASBC	Compressive strength (MPa)	Bending strength (MPa)	Compressive strength/ bending strength
Reference	44.2	7.1	6.2
AASBC(GUS)-0	43.9	6.2	7.1
AASBC(MS)-0	58.4	10.1	5.8
AASBC(GFA)-0	57.6	10.7	5.3

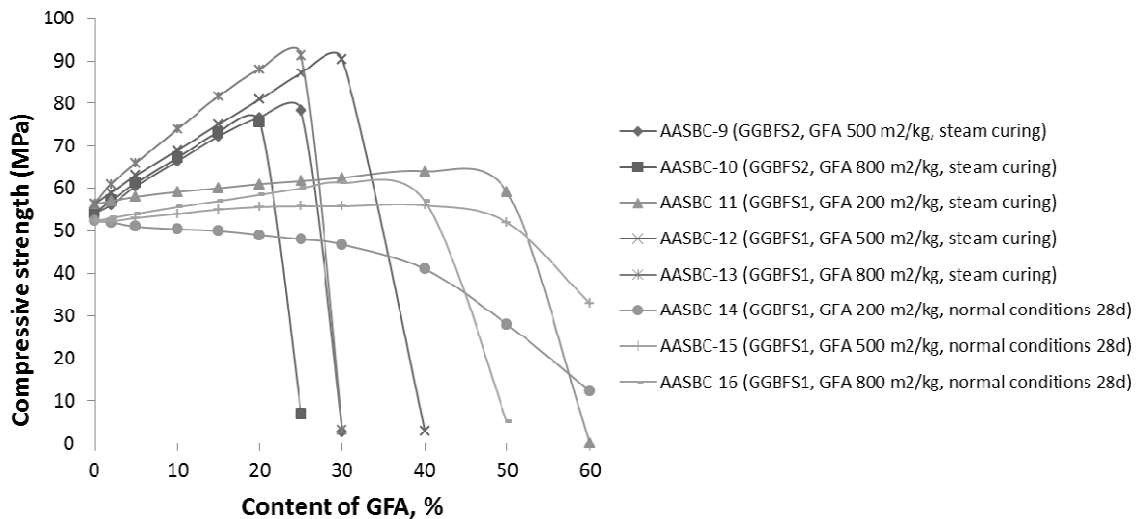


Fig.6 - The dependence of the strength of AASBCs (GFA) on the curing conditions, S_{sp} , and GFA content.

on the amount and fineness of the GFA. The setting times of the AASBC(GFA) when GFA with S_{sp} of 200, 500, and 800 m^2/kg was used increased by up to 1.5, 3, and 4 times, respectively (Table 3).

Influence of the GFA on the AASBC hardened paste

In general, glassy class F GFA has a low basicity and slow reaction to alkali at concentration of Na_2O 5% compared to GGBFS [23]. When GFA is added to GGBFS, the main component i.e. GGBFS is diluted. However, unequigranular, polymineral- and quarter-phase GFA (Table 2) combine the qualities of the reactive additive (fine particles of glassy GFA) and physically active blending material (quartz and mullite particles of different sizes). The GFA particles of medium and large sizes in the first stage proceeds are fillers and are additional aluminosilicate sources in blended AASBC(GFA)cement. The effect of the GFA on the strength of AASBC(GFA) depending on the S_{sp} , curing conditions, and GGBFS basicity is shown in Figure 6. When a GFA with a low S_{sp} of 200 m^2/kg (AASBC-11,14) is used, the "physical activity" of GFA predominates. An increase in the S_{sp} from 200 m^2/kg to 500 m^2/kg (AASBC-9,12,15) and 800 respectively (AASBC-10,13,16) facilitates the appearance of the pozzolanic reaction of the GFA.

Unlike physically active blending materials (GUS), GFA exhibits physical activity at a low S_{sp} , which is 1,5 times lower than that of GGBFS, only when steam curing is used (AASBC-11) (Figure 6). The permissible content of GFA of S_{sp} 200 m^2/kg when the strength of blended cement is comparable to that of the reference can reach 50% depending on the basicity of GGBFS when steam curing is used. The grinding of FA to reach an S_{sp} of 200 to 500 and 800 m^2/kg increases the content of particles of sizes below 5 μm by more than 30%, the solubility of GFA in the basic medium, and interaction with the mineral matrix of the AASC

[2,23,24]. An increment in the strength of the AASC mixed with GFA of S_{sp} of 500–800 m^2/kg (AASBC 9,10,12,13,15,16) at content 20-30% is up to 62%, depending on the basicity of GGBFS, curing conditions, and S_{sp} of GFA (Figure 6). GFA also becomes much more reactive at elevated temperatures than at room temperature; hence, the increment in strength after steam curing is higher and is up to 62% at GFA content of 25-30% and in normal conditions (28 days) up to 17% at GFA content of 20-25%. The effect of curing conditions on the strength of AASBC(GFA) is similar to that of blended OPC with siliceous materials - SCM.

The presence of the crystalline and glassy phases in GFA, the increase in the solubility in the mineral matrix when the GFA particles decrease in size at high temperature influence the dependence of the effect of GFA on the AASBC(GFA) strength. These factors contribute as much as GGBFS S_{sp} and basicity and curing conditions affect the properties of blended cements.

Increase in the pre-hardening time from 2 hours to 16 hours allows an increase in the GFA content and affects the strength (Figure 7). During pre-hardening at room temperature, the solubility of silica in AASBC (GFA) is low. During pre-hardening, when the admixture content is below the threshold value, a certain amount of calcium oxide from the GGBFS liberates into the intergranular space. This calcium oxide probably maintains the pH into the binder system at a sufficient high level. With increase of the temperature, the release rate of silica from GFA glassy phase increases significantly more rapidly than the dissolution of GGBFS, and pH value decreases to a crucial level at lower GFA content. With increase in the duration of the pre-hardening time from 2 to 16 h, the GFA content and strength of AASBC (GFA) increases (Figure 7).

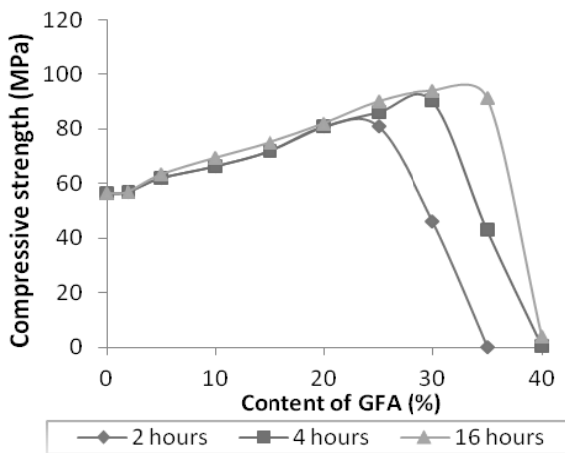
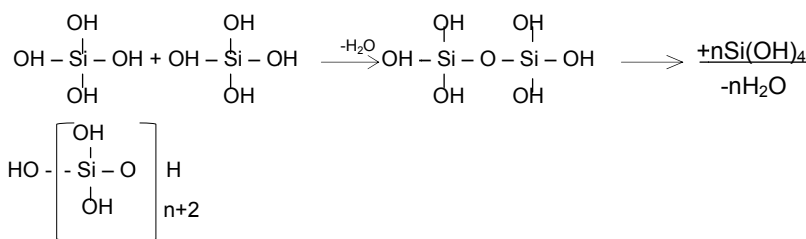
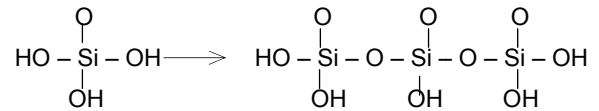


Fig. 7 - The dependence of the strength of AASBC-13 (GGBFS1, GFA 800 m²/kg, steam curing) on the pre-hardening time.

The strength of blended binder AASBC (GFA) abruptly decreases at a particular GFA content (Figure 6), especially when the samples are steam cured and when the $S_{sp} > 500 \text{ m}^2/\text{kg}$. Thus, the appropriate concentrations of GGBFS and GFA are limited, determined by the basicity of GGBFS, particle size of GFA, curing conditions, critical concentration of silica, and its transformation to orthosilicic acid-bound colloidal particles of hydrated silica. Hypothetically, this is caused by the mutual conditionality of threshold content of glassy silica and pH of the hardening binder system of AASBC. High-alkali medium of AASC promotes the reactivity of aluminosilicate glass in GFA [25]. The solubility of silica consists of simultaneous processes of hydration and depolymerization [26], which can be described by the total reaction: $(\text{SiO}_2)_n + 2n\text{H}_2\text{O} \leftrightarrow n\text{Si}(\text{OH})_4$. At a $\text{pH} < 8$, the solubility of silica is $2 \times 10^{-3} \text{ mol/L}$ and with an increase in the pH, the solubility increases up to 11 to 25 times. The solubility of silica at high pH increases because of the formation of $\text{Si}(\text{OH})_4$ and $[\text{Si}(\text{OH})_6]^{2-}$ [27]. Orthosilicic acid is unstable and is easily converted into a polymer by polycondensation even in very dilute solutions. Initially, the chain polycondensation takes place, and then with an increase in concentration or decrease of pH value, the chains are interconnected by the formation of a polysilicic acid gel [26-28] according to the following reaction.



Undissociated H_4SiO_4 is the major form of orthosilicic acid existence at $\text{pH} = 8$; at $\text{pH} = 12$, SiO_4^{4-} is the major form of existence [27]. At $\text{pH} = 8-11.71$ orthosilicic acid is in equilibrium with H_3SiO_4^- and with an ion $\text{H}_2\text{SiO}_4^{2-}$ at $\text{pH} = 11.71-12$. According to [29], monomeric H_3SiO_4^- is capable of polymerizing (condensing) in a very short period of time according to the following schematic process.



The small GFA particles consisting of reactive aluminosilicate glass introduce a significant amount of silicic acid into the intergranular spaces of the hardening cement. The entrance of an acid oxide (silicon oxide) leads to the disruption of the acid-base balance and the pH of the liquid medium of the cement begins to decline. When the pH of the solution reaches a certain level, the silicic acid ions polymerize in a very short period and the intergranular spaces of the hardening cement paste is filled with bound colloidal particles of hydrated silica. Hence, the compressive strength significantly worsens in comparison to the samples in which the FA content is lower than the critical limit. Simultaneously, the extraction from GGBFS calcium oxide (basic oxide) promotes an increase in the pH. Thus, the changes of the acid-base balance in the liquid phase of GFA-AASC system depend on the influencing factors of both rise and lowering of the pH of the medium. When the GFA content is lower than the permissible amount required for the silicic acid formation, which is insufficient for decrease the pH at a lower level than the critical value, polymerization ceases to occur and the mixed cement fresh paste hardens with the formation of a high-strength structure. In Figure 6, it can also be observed that the grinding of FA to achieve a $S_{sp} > 500 \text{ m}^2/\text{kg}$, although the S_{sp} of GGBFS is $300 \text{ m}^2/\text{kg}$, fails to lead to a considerable improvement in the strength characteristics of GFA-AASC. Hence, S_{sp} of $\sim 500 \text{ m}^2/\text{kg}$ is sufficient and is the upper limit for GFA in AASBC(GFA) based on neutral and acid GGBFS, activated by sodium carbonate.

Table 6

Ranges of replacement of GGBFS by GFA			
GGBFS	Curing conditions	Ranges of the replacement GGBFS by GFA	
		effective	permissible
GGBFS 1	normal conditions	up to 40-50% (FA S_{sp} 500-800 m ² /kg)	-
	steam curing	up to 50% (GFA S_{sp} =200 m ² /kg)	up to 30% (GFA S_{sp} =500-800 m ² /kg)
GGBFS 2	normal conditions	up to 30% (GFA S_{sp} 800 m ² /kg)	-
	steam curing	up to 30% (GFA S_{sp} 200 m ² /kg)	up to 30% (GFA S_{sp} =500-800 m ² /kg)

Table 7

Characteristics of fresh paste of the AASBCs with MS						
Content of MS in AASBC, %	GGBFS1			GGBFS2		
	Normal consistency, %	Setting time, hour-minute		Normal consistency, %	Setting time, hour-minute	
		initial	final		initial	final
0	24.9	1-20	3-50	25.8	0-50	3-00
1	23	1-10	3-40	23.9	0-40	2-50
3	20.8	0-45	2-50	21.5	0-30	2-30
5	19.5	0-45	2-30	19.9	0-25	2-20
7	19.0	0-40	2-10	19.7	0-25	2-10
10	18.8	0-40	1-50	19.5	0-25	2-10
20	18.7	0-45	2-00	19.4	0-35	2-30

With regard to the development of the compressive strength of AASBC(GFA), the introduction of GFA leads to a diminish of the early strength, although lesser than that determined of GUS (Figure 3). However, by introduction of GUS, the strength of GFA-AASC is nearly similar to that of the reference after 28 days age and after one year, AASBC(GFA) is superior than the reference and AASBC(GUS).

Combining the qualities of the filler and the reactive supplementary material, GFA can be a permissible and effective replacement of GGBFS. The results illustrate that GFA increases the strength of the AASC and can be used as a replacement of GGBFS by up to 50% (Table 6). As in the case of blended OPC, the effectiveness of supplements increases with increase in the basicity of the main constituent, curing temperature, and S_{sp} of the additives. The F_e of GFA is 0.9–1.6 depending on its S_{sp} .

For physically active and reactive GFA, the influencing factors affect the efficiency of GFA in the following order: (S_{sp} of FA, curing conditions, GGBFS basicity) > pre-hardening time.

The strength characteristics of AASBC(GFA)-0 mortars are presented in Table 5. The addition of 30% of GFA to AASC increases the compressive and bending strength of the mortars.

3.3. Reactive MS

The influence of MS on AASBC fresh paste

MS has a plasticizing effect on AASBC(MS) paste. The water requirement for additions of MS up to 20% decreases from 24.9–25.8% and 18.7–19.4% (Table 7). This is in agreement with the results obtained by Korolev [30]. As opposed to OC-based systems, the introduction of MS into

AASC does not increase water demand. We assume that the interactions in the GGBFS-MS- Na_2CO_3 solution binder system results in the “free” water release, leading to a plasticizing effect of MS.

The influence of MS on AASBC hardened paste

MS, due to its high reactivity exerts a significant positive affect on the compressive strength of AASBC(MS) binders (Figures 8 and 9 and Table 4).

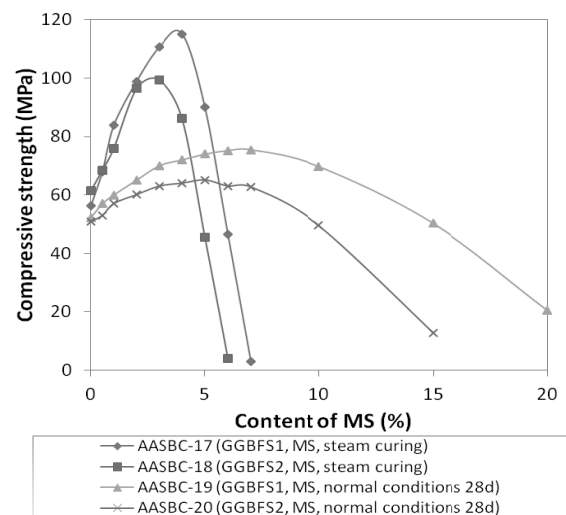


Fig. 8 - The dependence of the strength of AASBC(MS) on MS content, curing conditions, and GBFS basicity.

For reactive MS, the optimum addition and strengthening effect is determined by the curing conditions, the basicity of GGBFS, and pre-hardening time. The variation of the strength of AASBC(MS) binders with the MS content

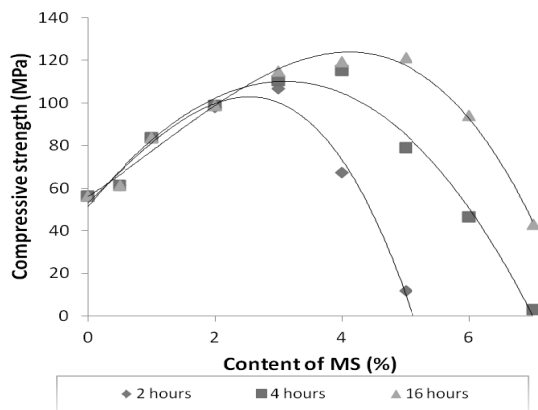


Fig. 9 - The dependence of the strength of AASBC (MS) AASBC (MS)-17 on the pre-hardening time.

resembles the gradation of that of AASBC(GFA) binders with GFA content of $S_{sp} = 500\text{--}800 \text{ m}^2/\text{kg}$. The GGBFS1 is more basic than GGBFS2. Hence, a 37% increase is seen in the compressive strength of MS-AASC binders cured in normal conditions when GGBFS1 is used and the increase is 27% when GGBFS2 was used (Figures 8 and 9). The upper limit of MS content is 7% for AASBC(MS) binders based on GGBFS1 and 5% for binders based on GGBFS2 when curing is carried out under normal conditions. For AASBC-(MS) binders based on GGBFS1, when cured under steam, the addition of MS leads to a compressive strength increase of up to 105% (115 MPa with 4% MS content) and for samples based on GGBFS 2, the increase is up to 60% (98 MPa with 3% MS content).

The strengthening effect of MS can be used for diminish the dosage of the alkali activator. MS exhibits strengthening effect on the AASBC(MS) binders. For early age of hardening three days and seven days, the compressive strengths of these binders are higher with up to 105 and 50 %, respectively, in comparison with the reference sample. After 360 days, the compressive strength of AASBC(MS) binders outbalances those of the reference AASC, the binders AASBC(GUS) and AASBC(GFA). However, the increment in the strength in percentage from 28 days to 360 days of the considered binders is minimum: about 28 % for AASBC - (MS) cured under normal conditions and 4.1 % for curing under steam (Figure 4).

For highly reactive additions, as in the case of MS, there are only certain effective AASC concentrations. The effective AASC quantities are 4% with steam curing and upto 7% under normal curing conditions. This is explained by the higher solubility of MS silica at higher temperatures encountered during steam curing than that under normal conditions. The significance of the influencing factors on the compressive strength of MS-AASC binders follows the order curing conditions > basicity of GGBFS > pre-hardening time. The value of F_e of MS is up to 1.9.

3.4. Structure formation process features, structure types, and structural elements of the AASBC hardened pastes

3.4.1. AASBC(GUS) binders

Despite the low chemical activity, GUS changes the hardening process of AASBC (GUS) from the moment of the mixing of GUS-AASC with an alkali activator solution. Because GUS does not react with alkali, the alkali solution to GGBFS ratio and Na_2O to $(\text{CaO}, \text{SiO}_2, \text{ and } \text{Al}_2\text{O}_3)$ the ratio increase in comparison with that of the reference AASC. Introduction of 30% GUS increases the concentration of Na_2O by GGBFS from 5% to 8%. The increased content of alkali metal oxide increases the activation and dissolution of GGBFS in the initial stages of hardening and the conditions are maintained over time. In addition, the supplementary alkali amount increases the surface erosion of the GUS particles, and the high pH prolongs the development of this process. Clearly, the eroded surface of the mechanically activated GUS has a high adhesion strength with the mineral matrix of AASC. In the process, the GUS particles facilitate the faster formation of hydrates in the interfacial zone during the later stages of the AASBC (GUS) hardened paste formation. This is indirectly confirmed by the development strength results of AASBC (GUS) up to 360 days (Figure 3b).

Studies on the interface between the AASC cement fresh paste and quartz sand in alkali-activated slag mortars [20, 31] have showed the formation of the strong, dense, and uniform interfacial transitional zones in comparison with OPC. Also, traces of chemical reactions [21] and the results of our studies seem to indicate the formation of a developing interfacial transitional zone. Evolution of this developing interfacial transitional zone over time causes an increase in the adhesion strength, which is because of a release of the surface GUS particles caused by gradual erosion at the high pH of the AASC mineral matrix. The structure of AASBC (GUS) hardened paste consists of three structural elements (Figures 5, 10a), including the mineral matrix of AASC, the developing interfacial transitional zone, and the GUS particles.

3.4.2. AASBC(GFA) binders

Polymineral and polyphase composition of FA causes a more complicated formation of the AASBC (GFA) hardened paste with a structure consisting of a larger number of elements. GFA affects the structure formation process at all stages of hardening and the participation of the components at every stage depends on the GFA particle size and its structure.

Since GFA contains crystalline material (22–29% - quartz and mullite), when mixing AASBC (GFA) with an alkali solution, the alkali solution to GGBFS ratio slightly increases. This intensifies the

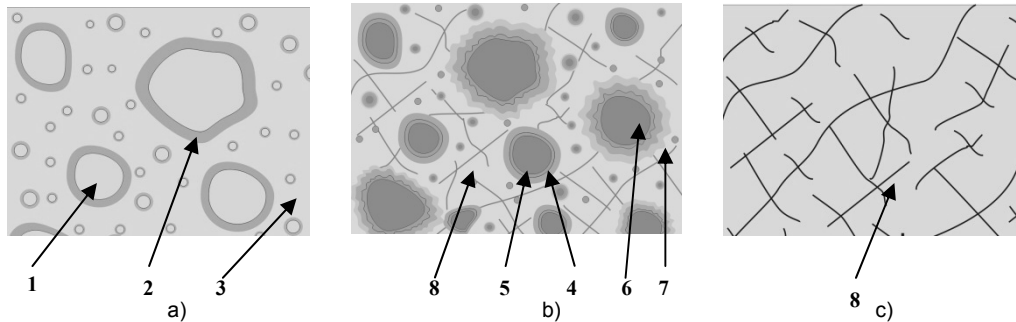


Fig. 10 - Structure types and structural elements of the AASBC hardened paste with physically active (a), physically active and reactive blending materials (b), and reactive supplements (c). 1 is GUS, 2 and 5 are the developing interfacial transitional zones, 3 is the mineral matrix of AASC, 4 is the crystalline GFA particle, 6 is the amorphous GFA particle, 7 is the interpenetrating interfacial transitional zone, and 8 is the skeleton.

gradual hydration and dissolution of GFA in the early stages of hardening and the continuation of this process during the time with GGBFS and GFA particles of larger sizes. GFA particles of sizes >5 mm, together with the crystalline GFA grains can act as nucleation sites for the reaction products. During the time, there is gradual loosening of the surface of the GFA particles, resulting in the erosion of the interfacial transitional zone, expansion of interpenetrating constituents, including the GGBFS and GFA-based hydration products. Corrosion of the surface of GFA particles after one day of hydration and hydration products at the edge around the GFA particles containing amorphous alkaline aluminosilicate hydrates have been observed before [32, 33]. Hence, the interfacial transitional zone between the AASC fresh paste and GFA particles of glass structure can be called as "interpenetrating." The slower reaction with the alkali component in comparison with GGBFS and the strengthening over time of the two types of interfacial transitional zones (developing and interpenetrating) create favourable conditions for strength increase of AASBC(GFA) binder at long periods of time (Fig. 3b).

GFA particles with sizes $< 5 \mu\text{m}$ exhibit high reactivity even for early stages of AASBC (GFA) binder hardening. It is assumed that the amorphous silica dissolved from the GFA glassy phase removes the Ca^{2+} from the GGBFS grains. The extraction of Ca^{2+} from GGBFS to the solid phase shifts the chemical equilibrium between the oxides in the direction of maintenance of a high concentration of Na_2O , resulting in the latter continuing to activate the GGBFS to achieve the equilibrium conditions of the component concentrations, typical for reference AASC. In addition, as a result of the cation exchange $2\text{Na}^+ \rightarrow \text{Ca}^{2+}$ in the liquid medium, caustic alkali is formed. There is a strong possibility that this alkali reacts with amorphous silica with sodium silicate formation, the anionic constituent of which is similar to the primary products of dissolution in the alkali aluminosilicate source, which serves as their

additional reserve. Krivenko [34] has observed that the chemical activity of GGBFS is defined by the amount of vitreous phase and pH and also the presence of the additives, which are capable of reacting with the hydrolysis products of the GGBFS glass and forming a crystalline skeleton of the hardened cement hardened paste. It is probable that GFA increases the reactivity of GGBFS. The introduction of GFA may lead to the additional activation of GGBFS, increasing the concentration of dissolution products of the starting materials and the volume of low-basic calcium silicate hydrates at the early stages of the hardening process, which reinforces the mineral matrix of AASC hardened paste and results in increased compressive and bending strengths (Table 3). Thus, the structure of the GFA-AASC hardened paste consists of three structural elements (Figure 10b) including, the mineral matrix with reduced basicity of the hydration products [21], a developing interfacial transitional zone, an interpenetrating interfacial transitional zone, crystalline, and amorphous FA particles. Figure 11a shows partly reacted fly ash particles in the volume of the binder gel, interfacial zone.

3.4.3. MS-AASC binders

MS shows extremely high reactivity, showing reactivity from early stages of hardening of AASBC (MS) binders. The MS action mechanism is analogous with those of the FA fine particles consisting of aluminosilicate glass (Figs. 6–9). The reactive MS binds with Ca^{2+} solubilised from GGBFS in the calcium silicate hydrates [30], forming a reinforcing skeleton of AASBC(MS) hardened paste. Figures 11b,c show that this skeleton penetrates the binder gel. Hence, the AASBC(MS) binders show the highest compressive and bending strength characteristics of AASBCs from an early stage of hardening.

The structure of AASBC (MS) hardened paste consists of structural elements (Figure 10c) including the mineral matrix with reduced basicity of the hydration products and the skeleton.

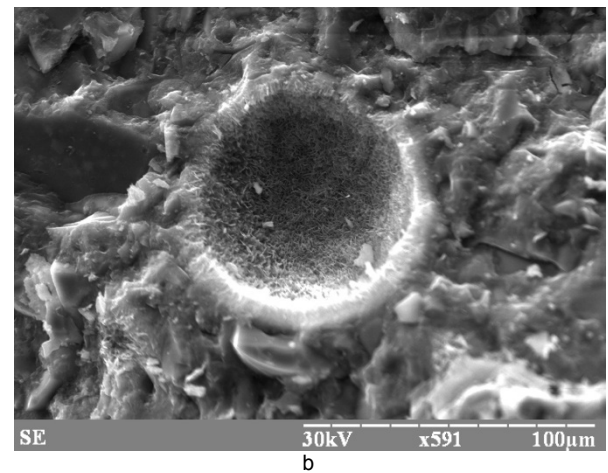
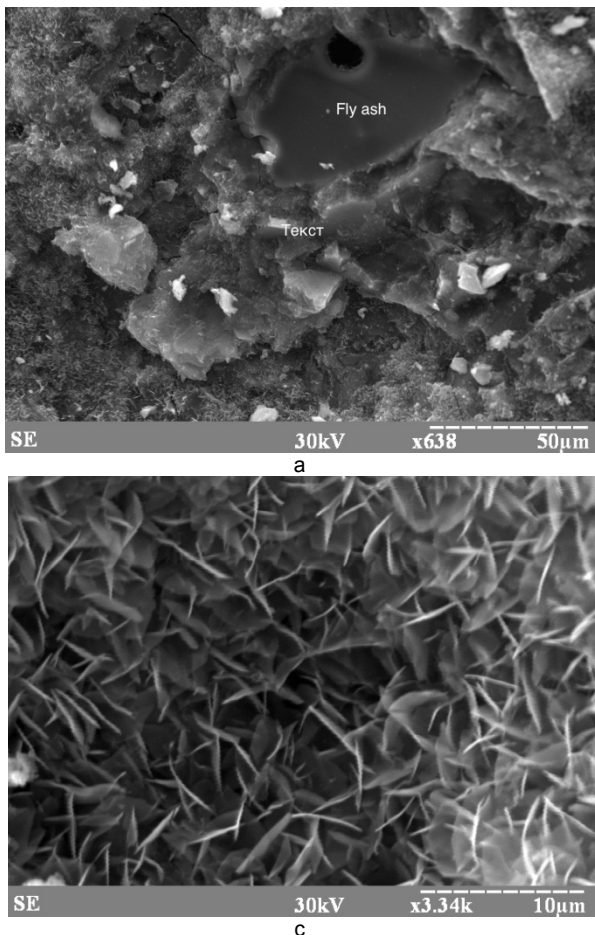


Fig. 11 - Scanning electron images of the hardened AASBC hardened pastes a) and b) AASBC (GFA), and c) AASBC (MS).

4. Conclusions

The results of the study are summarized in the following conclusions.

1. The effect of the siliceous mineral supplementary materials on the properties of fresh and hardened AASBCs properties depends on the activity, content and fineness of blending materials (GUS, GFA, MS), GGBFS basicity, curing conditions, and pre-hardening time.

2. The admixtures GUS, GFA (class F), and MS are effective for strength improvement of AASBC based on neutral and acid GGBFS, activated with sodium carbonate solution. The effectiveness factor values for GUS, GFA, and MS are 0.9–1.14, 0.9–1.6, and 1.9, respectively.

3. GUS and GFA are also effective for GGBFS replacement up to 50% in AASBC. Appropriate S_{sp} of GUS for AASBC is higher than $500 \text{ m}^2/\text{kg}$ and the upper limit of S_{sp} of GFA is $500 \text{ m}^2/\text{kg}$.

4. The influencing factors affect the strength of the AASBC in the following order:

- When introducing GUS - S_{sp} of GUS > (GGBFS basicity, curing conditions, and pre-hardening time).

- When introducing GFA - (S_{sp} of GFA, curing conditions, GGBFS basicity) > the pre-hardening time.

- When introducing MS - curing conditions > basicity of GGBFS > pre-hardening time.

5. The structural elements of AASBCs hardened pastes are as follows:

- With physically active blending materials (i.e. GUS), the elements are the mineral matrix of AASC, particles of blending material, and the developing interfacial transitional zone.

- With physically active and reactive blending materials (i.e. GFA), the elements are the mineral matrix of AASC, particles of crystal and amorphous structure of the blending material, developing and interpenetrating interfacial transitional zones, and skeleton.

- With reactive admixtures (i.e. MS), the elements include the mineral matrix of AASC and the skeleton.

REFERENCES

1. K.L. Scrivener, A. Nonat, Hydration of cementitious materials, present and future, *Cement and Concrete Research*, 2011, **41**, 651.
2. N.R. Rakhimova, R.Z. Rakhimov, A review on alkali-activated slag cements incorporated with supplementary materials, *Journal of Sustainable Cement-Based Materials*, 2014, **3**(1), 61.
3. B. Lothenbach, K.L. Scrivener, R.D. Hooton, Supplementary cementitious materials, *Cement and Concrete Research*, 2011, **41**, 1244.
4. M.A. Smith, G.J. Osborne, BFS/Fly ash cements, *Journal of World Cement Technology*, 1977, **8**(4), 223.
5. M. Tang, Optimum mix design for alkali-activated slag-high calcium fly ash concrete, *Journal of Shenyang Architecture and Civil Engineering Institute*, 1994, **10**(4), 315.

6. F. Puertas, S. Martínez-Ramírez, S. Alonso, Alkali-activated fly ash/slag cements: Strength behaviour and hydration products, *Cement and Concrete Research*, 2000, **30**(10), 1625.
7. C. Lu, The research and the reactive products and mineral phase for FKJ cementitious material, In Proceedings of 9th International Congress on the Chemistry of Cement, New Delhi, India, III, 1992, 319–324.
8. D. Li, J. Shen, Y. Chen, et al., Study of properties on fly ash–slag complex cement, *Cement and Concrete Research*, 2000, **30**(9), 1381–1387
9. C. Lu, The preliminary research of the fly ash-slag-alkali concrete, in Proceedings of 2nd Beijing International Symposium on Cements and Concrete, Beijing, 1989, **2**, 232.
10. J.L. Provis, R.J. Myers, C.E. White et al., X-ray microtomography shows pore structure and tortuosity in alkali-activated binders, *Cement and Concrete Research*, 2012, **42**(6), 855.
11. T. Yang, X. Yao, Z. Zhang et al., Mechanical property and structure of alkali-activated fly ash and slag blends, *Journal of Sustainable Cement-Based Materials*, 2012, **1**(4), 167.
12. N. Marjanović, M. Komljenović, Z. Baščarević, et al. Physical–mechanical and microstructural properties of alkali-activated fly ash–blast furnace slag blends, *Ceramics International*, 2015, **41**(1), 1421.
13. C. Shi, R.L. Day, Early strength development and hydration of alkali-activated blast furnace slag/fly ash blends, *J. Adv. in Cem. Res.* 1999, **11**(4), 189.
14. F. Puertas, A. Fernandez-Jimenez, Mineralogical and microstructural characterization of alkali-activated fly ash/slag pastes, *J. Cem. and Concr. Compos.*, 2003, **25**, 287.
15. S. Puligilla, P. Mondal, Role of slag in microstructural development and hardening of fly ash-slag geopolymer, *Cement and Concrete Research*, 2013, **43**, 70.
16. T. Yang, X. Yao, Z. Zhang et al., Mechanical property and structure of alkali-activated fly ash and slag blends, *Journal of Sustainable Cement-Based Materials*, 2012, **1**(4), 167.
17. N.R. Rakhimova, R.Z. Rakhimov, Properties and structure formation of a stone of compositional slag alkaline bindings with siliceous mineral additives In Proceedings of the XIII International Congress on the Chemistry of cement, Madrid, July 2011, edited by Á. Palomo, A. Zaragoza, J.C.L. Agüí, p.200.
18. N.R. Rakhimova, R.Z. Rakhimov, Properties of alkali-activated slag cements, *Zement-Kalk-Gips International*, 2012, **11**, 32.
19. V.D. Glukhovskiy. Slag-alkali Cements and Concretes, Vysscha Shkola Publisher, Kiev, 1978.
20. C. Shi, P. Xie, Interface between cement paste and quartz sand in alkali-activated slag mortars, *Cement and Concrete Research*, 1998, **28**, 887.
21. J. Deja, Carbonation aspects of alkali activated slag mortars and concretes, *J. Silicates Industriels*, 2002, **67**, 37.
22. H. Xu, J.L. Provis, J.S.J. Van Deventer, P.V. Krivenko, Characterization of aged slag concretes, *ACI Mater. J.*, 2008, **105**, 131.
23. N.R. Rakhimova, Dr thesis, Alkali-activated slag cements and concretes with silica and silica-alumina additives, Kazan State University of architecture and engineering, Russian Federation, 2010.
24. J. Benezet, A. Benhassaine, The influence of particle size on the pozzolanic reactivity of quartz powder, *Powder Technology*, 1999, **103**, 26.
25. V.D. Glukhovskiy, P.V. Krivenko, P.V. Starchuk, Alkali-activated slag concretes based on fine-grained aggregates, Higher school, Kiev, 1981.
26. V.V. Gerasimov, Inorganic polymers based on silicon and phosphorus oxides, Stroiizdat, Moscow, 1993.
27. R. Ailer, Chemistry of silica, World, Moscow, 1982.
28. V.I. Korneev, Manufacture and application of water glass, Stroiizdat, Leningrad, 1991.
29. V.B. Tolstoguzov, Inorganic polymers, Science, Moscow, 1967.
30. V.A. Korolev, Binder, USSR Author's certificate No.161516, 1990.
31. V.P. Ilyin In Proceedings of the 1st International Conference on Alkaline Cements and Concretes, Kiev, 1994.
32. C. Shi, R.L. Day, Early strength development and hydration of alkali-activated blast furnace slag/fly ash blends, *Advances in Cement Research*, 1999, **11**(4), 189.
33. F. Puertas, A. Fernandez-Jimenez, Mineralogical and microstructural characterization of alkali-activated fly ash/slag pastes, *Cement and Concrete Composites*, 2003, **25**, 287.
34. P.V. Krivenko, Mechanisms of the structure and property formation process of alkali-activated cement stone, *Cement (in Russian)*, 1985, **3**, 13.
